Proceedings of the 11th International Conference

PRIP'2011

Pattern Recognition and Information Processing

18–20 May 2011, Minsk, Belarus

Belarus, Minsk

UDC 004.93'1
BBC 32.973.26–018.2
P32

Pattern Recognition and Information Processing (PRIP'2011) : proceedings of the 11th International Conference (18 – 20 may, Minsk, Republic of Belarus). – Minsk : BSUIR, 2011. – 472 p.
ISBN 978-985-488-722-7

The book collects the papers accepted for publication and presentation at the 11th International Conference on Pattern Recognition and Information Processing (PRIP'2011) that will be held at may 18 – 20 in Minsk, Belarus. The proceedings are prepared for publication by PRIP'2009 Program Committee and Belarusian Association for Image Analysis and Recognition .

Proceedings will be useful for students and researchers working in the following areas: pattern recognition and image analysis; knowledge processing and representation; knowledge based decision support system, fuzzy mathematics and systems, applications of pattern recognition and image analysis.

Papers are reviewed by at least two reviewers and approved by Program Committee. All papers have been photographically reproduced exactly as submitted by authors on their own responsibility.

UDC 004.93'1
BBC 32.973.26-018.2

Contributors PRIP'2011

Conference is organized by:

- Belarusian State University of Informatics and Radioelectronics

in cooperation with:

- United Institute of Informatics Problems of the National Academy of Sciences of Belarus
- Belarusian State University, Faculty of Applied Mathematics and Computer Sciences
- Belarusian Association for Image Analysis and Recognition
- Enterprise IT-Park
- Bluemedia Ltd.
- Effective Software Ltd.
- Enterprise ISsoft Solutions
- Enterprise TelesoftService
- Syncsis Ltd.

in colloboration with:

- Belarusian Republican Foundation for Fundamental Research
- International Associations for Pattern Recognition

Section list

Contents

Object extraction at nano-surface images

A. Nedzved[1], O. Nedzved[2], S. Ablameyko[1], S. Uchida[3]
1) United Institute of Informatics Problems of the National Academy of Sciences, Belarus. e-mail: abl@newman.bas-net.by
2) Belarusian State Medical University, Belarus, e-mail: olga_nedzved@tut.by,
3) IS Dept, Kyushu University, Japan. e-mail: uchida@is.kyushu-u.ac.jp

1. INTRODUCTION

Recently with fast development of nano-teechnologies, atomic force microscopy (AFM) are started widely used. They allow determining the sizes of structural elements and mechanical properties of objects at nano-surfaces [1]. The individual atoms, molecules and large macro-associations are considered in studying the characteristics of nano-scale objects.

However, further image analysis methods should be used to extract objects and their characteristics. This is quite difficult task because nano-surface images have many specifics. There are attempts to process such type or similar images [2-5]. However, each concrete case should be considered in details. We considered processing magneto-optical images in our papers [6-7]. This study continues analysis of magneto-optical images moving to nano-surface images.

In the paper, the processing scheme, methods of constructing finite element models of nano-samples of AFM images, setting rules of the boundary conditions for simulation of contact interaction are proposed. The results of computational experiments to determine the characteristics of image objects by means of the package LS-DYNA are presented.

2. SPECIFICS OF NANO-SURFACE IMAGES

The nano-surface objects can be represented as hemispheres. They are presented as rounded regions with increasing brightness toward the center on grayscale nano-images (Figure 1).

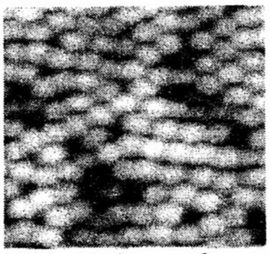

Fig. 1 – Grayscale image of nano-surface with spherical objects

The brightness profile of the original image horizontally is represented by a smooth line (Figure 2). A profile in the vertical direction has high contrast and small overshoots (Figure 3).

There is a heterogeneous geometric contrast on the image where the vertical changes component is much higher than horizontal component. This effect is related to the conditions of imaging. The process of constructing an image is based on scanning the surface of the cantilever. After scanning, at the image the duration of receipt of the adjacent vertical pixels is significantly higher than the duration of receipt of horizontal pixels. The result is affected by a number of external interference: a geometric drift and the drift of brightness.

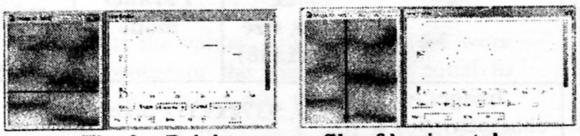

Fig. 2 – Brightness profile of horizontal and vertical direction

Also a cantilever has a certain inertia in the time of the horizontal scanning. This causes to the fact that the properties of light in each line receive the unique features. Such heterogeneity is reflected in the global brightness histogram (Figure 3). Histogram of the nano-surface is similar to a Gaussian distribution. But it has a lot of individual pulses that sharply differ from their neighbors. A removing or compensation for these defects is necessary because they affect the quality of image processing.

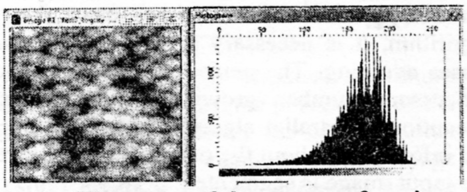

Fig. 3 – Histogram of the nano-surface image

3. CORRECTION OF LOCAL CONTRAST HETEROGENEITY

Geometric heterogeneity of the contrast in images obtained by atomic force microscopy is a serious problem which solution in the general case has not yet been found.

In this paper, we propose two approaches. The first one is to generate a possible background for the image, the second is based on the calculation of the characteristics of local contrast for vertical and horizontal lines. Both approaches are based on the assumption of symmetry of objects at the nano-surface.

In the first method, two background images are generated. One is created by repeated application of a simple averaging convolution with a large raster (for 256x256 image – bitmap 14x14):

$$I_{xy} = \frac{1}{2 \cdot n} \sum_{i=y-n}^{y+n} \sum_{j=x-n}^{x+n} I_{ij}$$

where I_{xy} – value of the pixel on the image with coordinates x, y, n – the half-size of the raster convolution.

As a result of this transformation an image corresponding to dark backgrounds is obtained (Figure 5. b).

M be a spectral endmembers matrix of $l \times m$ dimension. Linear mixture model is described by the equation

$$r = M \times \alpha + n \quad (1)$$

where $\alpha = (\alpha_1, \alpha_2, .. \alpha_l)^T$ – vector of $l \times 1$ dimension, α_j – fraction of j-th endmember in pixel, n – vector of $m \times 1$ dimension, which describes the additive noise. Vector α is an approximate solution to the overdetermined equation $M \times \alpha \approx r$. Endmember fractions in (1) are the solution to simultaneous equations

$$\begin{cases} \| M \times \alpha - r \| \to \min \\ \sum_{j=1}^{l} \alpha_j = 1 \\ \alpha_j \geq 0 \ \forall j = 1,..l \end{cases} \quad (2)$$

where the constraints imposed by physical considerations.

In [5] a faithful algorithm for (2) solving is presented. Unfortunately, this model is rarely realized in practice, because the full matrix of endmembers of scene is usually unknown. In this case, there is one or more reference endmembers extracted, and the rest treated as junk. In [6] known algorithm of such type TCMI is extended to the case of physical constraints over endmember fractions:

$$\begin{cases} (r - M \times \alpha)^T \times R^{-1} \times (r - M \times \alpha) \to \min \\ \alpha_j \geq 0 \ \forall j = 1,..l \end{cases} \quad (3)$$

where $R = \sum_{i=1}^{n} r_i \times r_i^T$, n is the number of pixels in image, which is analyzed.

Subpixel analysis is a powerful tool for many remote sensing applications. However, the allocation of each endmember within the pixel remains uncertain. But if you adjust the correct allocation of endmember fractions inside the image pixels in view of spatial relationships, and then perform the endmember fractions mixing yet in the image subpixels, you can get enhanced hyperspectral image.

Generally, natural and artificial objects of the Earth's surface follow the principle of compactness, i.e. subpixel fractions of the same endmember in adjacent pixels often also spatially located in the adjacent subpixels. Therefore it is possible to reallocate subpixel fractions α_{iq}, $q = 1, .. k$, within each pixel in a certain optimal way. In this case, the endmember total fraction α_i within a whole i-th pixel must be kept:

$$\sum_{q=1}^{k} \alpha_{iq} = k\,\alpha_i \quad (4)$$

where k – the number of subpixels per pixel.

After the reallocation of subpixel fractions for all l endmembers present in the current pixel, the full signal r_{iq} in each q-th subpixel can be calculated as a mixture of endmember spectra M_j, $j = 1, .. l$, with weights of corresponding subpixel fractions:

$$r_{iq} = \sum_{j=1}^{l} \alpha_{ijq} \cdot M_j \quad (5)$$

Mixing (5) consistently runs for all k subpixels of all n pixels in image and thus a subpixel spatial resolution hyperspectral image is formed [9].

4. ALGORITHM

A specific feature of the future Belarusian and Ukrainian remote sensing satellites is the simultaneous acquisition both multispectral and hyperspectral imagery with different spatial resolution. This feature can be used for joint sub-pixel analysis of remote sensing data, while the spectral endmembers unmixing is carried out by hyperspectral imagery, and higher-resolution multispectral one handles as reference for the reallocation of subpixel fractions. So, the new algorithm for hyperspectral imagery spatial resolution enhancement based on reallocation of subpixel spectral endmember fractions is offered. The processing dataflow is shown in Fig.1.

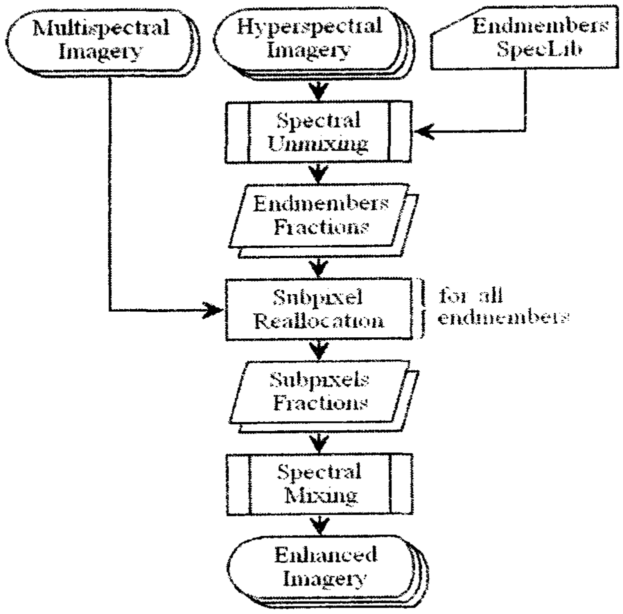

Fig.1 – Joint subpixel analysis flowchart

In hyperspectral image the endmembers unmixing is performed according to (3). The spectral reflectances of endmembers are stored in the spectral library. In such a manner the endmember fractions are traced in hyperspectral image pixels. Further, taking into account the endmember subpixel fractions spatial relationships and constraints (4), a reallocation of endmember subpixel fractions in subpixels of each pixel of the hyperspectral image is carried out by reference to higher resolution multispectral image. This operation is performed for all endmembers and thus the subpixel fractions thereof are obtained. In conclusion, reallocated endmember fractions in subpixels are mixed up by (5), resulting in hyperspectral image of enhanced spatial resolution. Hyperspectral image scaling ratio in the processing is caused by the number of subpixels per pixel k, i.e. by the source and reference images resolution quotient.

It is obvious that the visual and interpretational accuracy of the enhanced resolution restored image will depend both on the correct endmembers identification in the reference image, and analysis completeness of all endmembers present in the scene.

$$\bar{L}^*(i,j) = \bar{L}(i,j) + \left(\frac{C^*(i,j) * n * m}{1 - C^*(i,j)} - \sum_{\forall (i,j) \in W_k - W_l} \left(\bar{L}(i,j) - L(i,j) \right)^2 H\left(L(i,j)\right) \right)^{0.5}$$

This procedure is repeated for each element of each horizontal image line.

The proposed algorithm uses the statistical definition of local contrast. Due to this the homogeneity of texture, its "roughness" and granularity are taken into account (Figure 7).

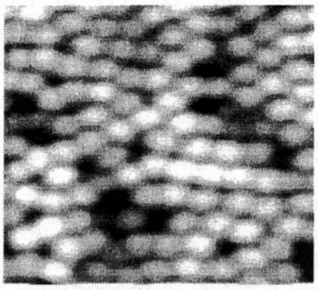

Fig. 7 – The result of the local correction of the contrast on the image of nano-surface

The experiment showed that the second method gives a clearer picture as a result, but the first method works three times faster.

4. OBJECT EXTRACTION AT NANO-SURFACE IMAGES

Objects that form the surface are the basis for determination of its characteristics: size, shape, height and position. To determine these characteristics is it necessary to find applicable objects in the image.

The selection of objects can be carried out in different ways. We assume that the objects are presented as spheres that intersect. In this case they can be represented as a topological surface. Then it is possible to determine the position of cavities between them.

4.1 WATERSHED-BASED IMAGE SEGMENTATION

Watershed algorithm is used for determining the boundary lines between objects. The resulting image is often divided into a large number of small areas (pools), most of which are not significant in solving the problem.

Lines of the watershed of the image are the boundaries that separate areas of this image. In the topographic representation of images, numerical values (such as gray levels) for every pixel serve as the height of this point. The main problem of this algorithm is over-segmentation, because all boundaries and noises are displayed in the gradient. Therefore the process of noise removal is necessary.

As a result the direct application of this algorithm to the image of nano-surface gives additional false objects (Figure 8).

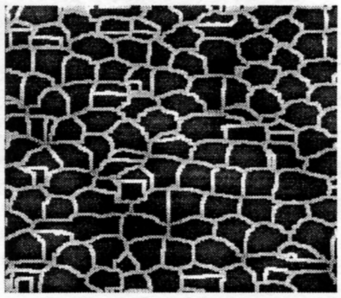

Fig. 8 – Result of the algorithm watershed applied directly to the image of nano-surface

Application of contrast correction before the noise filtering significantly improves the result (Figure 9).

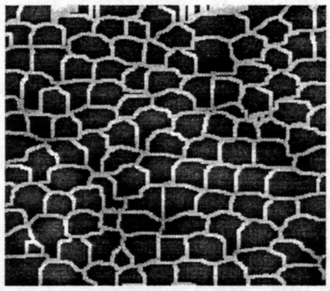

Fig. 9 – The result of watershed algorithm applied to image of the nano-surface after local contrast correction and a noise filtering

The algorithm allows obtaining the boundary of objects. However, the boundary lines are slightly chopped because a transformation uses urban metrics of computation of distances.

4.2 OBJECT EXTRACTION AT SEGMENTED IMAGE

As mentioned above the objects in the image represent hemispheres but the image boundaries mainly composed of polygons. To solve this problem, a special algorithm for correcting the shape on the basis of mathematical morphology was developed.

The first step of algorithm is the the inversion of boundaries Then objects clasped to the edge are removed (Figure 10).

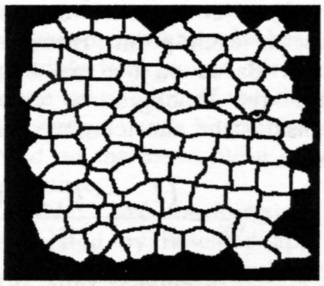

Fig. 10 – The result of removing of objects clasped to the edge

The image contains small objects that have emerged in the empty fields. They are removed by a noise filtering by area (Figure 11).

Then the correction of boundaries of objects by using morphological opening operation is performed (Figure 12).

In the result objects of nano-surface image are extracted. This algorithm has several advantages compared with the original method. It allows to extract objects and calculate the series of geometric and brightness characteristics which can be used for a more complete description.

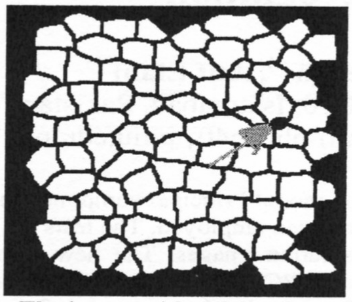

Fig. 11 – The image with a deleted small object

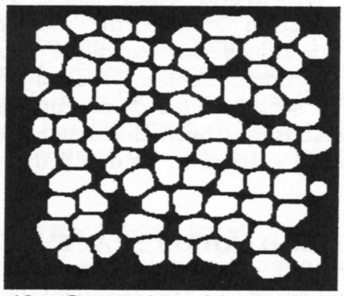

Fig. 12 – Correction of form of objects

5. CONCLUSION

In the paper, the scheme of computational experiments, methods of constructing finite element models of nano-samples of their AFM images, setting rules of the boundary conditions for simulation of contact interaction have been proposed. The results of computational experiments to determine the characteristics of contact interaction by means of the package LS-DYNA were presented. The obtained results show that it is possible to extract images objects and calculate the series of geometric and brightness characteristics and image features in such complicated images as nano-structures.

6. REFERENCES

[1] Sellmyer, D. Advanced Magnetic Nanostructures / D. Sellmyer, R. Skomski. – Springer, 2006. – 514 p.

[2] Szmaja, W. "Digital Image Processing System for Magnetic Domain Observation in SEM"/ W. Szmaja // J. Magnetism Magnetic Mater. – 1998. – No. 189(3). – 353-365 p.

[3] M. Yukio, I. Hisafumi, and K. Hitoshi, "Automatic Visual Inspection System for Thin Film Magnetic Head Wafer Using Optical Enhancement and Image Processing Technique," in Proc. SPIE Applications of Digital Image Processing XV, Ed. by A. G. Tescher (SPIE Homepage) 1771, 20 (1993).

[4] Q. Zhu, X. Wang, X. Zou, et al., "Feature Extraction for Magnetic Domain Images of Magneto-Optical Recording Films Using Gradient Feature Segmentation," J. Magnetism Magnetic Mater. 248(2), 292 (2002).

[5] L. Wang, Z. Fan, and D. E. Laughlin, "Trace Analysis for Magnetic Domain Images of L10 Polywinted Structures," Scripta Materiala 47(11), 781 (2002).

[6] P. Paturi, LarsenB. Hvolbaek, B. Jacobsen, and N. Andersen, "Image Correction in Magneto-Optical Microscopy," Rev. Sci. Instr. 74(6), 2999 (1990).

[7] A. Nedzved, S. Ablameyko, M. Tekielak, et al., Processing of Needkes-Like Images of Magnetic Domain Structures in Ultrathin Cobalt Wedge, 8th International Conf. on Pattern Recognition and Information Processing (PRIP'2005), May 18–20, 2005, Belarus, Minsk (2005), pp. 108–111.

[8] Nedzved A., Dobrogowski W., Ablameyko S., Tekielak M. and Maziewski A. Analysis of nanostructures by magneto-optical images // Pattern Recognition and Image Analysis, Vol. 19, N.2, 2009, P. 321-333